Evaluation of the Effect of Future Climate Change on the Distribution and Movement of Moisture in the Unsaturated Zone at Yucca Mountain, Nevada

by A.C. Ritcey[a], Y.S. Wu[a] and G.S. Bodvarsson[a]

[a]Earth Sciences Division, Lawrence Berkeley National Laboratory, Berkeley, California, 94720 U.S.A.

Abstract

The objective of this paper is to predict the effect of changes in future climatic conditions on the distribution and movement of moisture in the unsaturated zone (UZ) at Yucca Mountain. Modeling is conducted using TOUGH2, a multiphase, integrated finite difference numerical model (Pruess, 1991) calibrated using available saturation, water potential and pneumatic data from six boreholes. Modeling results indicate that future climatic conditions may increase lateral diversion above low permeability units of the Calico Hills nonwelded (CHn) hydrogeologic unit and decrease lateral diversion above the Paintbrush nonwelded (PTn) hydrogeologic unit. The existence of lateral diversion above the CHn hydrogeologic unit is important because additional water flux due to increased infiltration may not travel through altered zeolitic layers, therefore decreasing the potential of radionuclides released from the repository to be sorbed by these layers. Collection and analysis of additional geochemical data will decrease uncertainty in capability of the PTn and altered CHn hydrogeologic units to create barriers to vertical flow, and therefore improve confidence in future climatic predictions.

Keywords: Unsaturated-Zone; Hydrology; Climate; Modeling

1

1. Introduction

The goal of this study is to predict the impact of future climatic changes on moisture distribution and movement using a 3-dimensional (3-D) numerical model specifically developed for the UZ at Yucca Mountain (Wittwer et al., 1995; Bodvarsson and Bandurraga, eds., 1996; Bodvarsson et al., eds., 1997). The future climate may change for a variety of reasons, including volcanic eruptions, continental drift and other earth-scale phenomena, cyclical changes in the earth's orbital parameters, and changes due to burning of fossil fuels and other anthropogenic activity (Forester et al., 1996; Schelling and Thompson, 1997). Wetter and cooler climates are likely to increase the quantity and spatial distribution of precipitation, and may affect parameters such as vegetation, evapo-transpiration, soil thickness and hydrologic properties. In this study, surface and near-surface conditions have been considered aggregately by modeling future climate using only changes in net infiltration. Nevertheless, because net infiltration is a dynamic process that affects the movement of water, gas, and heat in the UZ, it is key to understanding how climatic changes may affect subsurface conditions and processes. Previous numerical studies using future climatic conditions in the UZ at Yucca Mountain include Sonnenthal and Bodvarsson (1997) who modeled chloride geochemistry using climate conditions from 21,000 years ago (21-ka) which are expected to be similar to future climatic conditions, and Wu et al. (1996), who modeled the movement of a high infiltration pulse through the UZ at Yucca Mountain using a dual-permeability model.

2. Modeling Approach

2.1 Climate Scenarios

One important factor in modeling future climate is selecting climate scenarios that adequately capture the range of expected conditions. This study considers two future climate scenarios: a two-fold increase in infiltration resulting from a doubling of atmospheric carbon dioxide (CO_2) concentrations due to anthropogenic activity (herein referred to as the "2x CO_2 scenario"), and a five-fold increase in infiltration approximately corresponding to the most recent glacial period which reached a maximum 21-ka (herein referred to as the "21-ka pluvial scenario"). Higher infiltration may also have occurred from 120 to 150 ka when the polar ice sheets extended even further than during the maximum at 21-ka (Smith, 1984; Winograd et al., 1988, 1992; Jannick et al., 1991; Szabo et al., 1994; Tyler et al., 1996). Schelling and Thompson (1997) indicate that burning of fossil fuels may increase CO_2 by as much as six times, causing drier conditions and substantially lower infiltration rates than were considered in this paper.

Estimates of precipitation are based on the U.S. Geological Survey's (USGS) work using National Center for Atmospheric Research (NCAR)'s regional climate model code (RegCM2) (Schelling and Thompson, 1997). An important input for the RegCM2 model is the location of the jet stream, which are the steering winds for precipitation. The 21-ka pluvial scenario, which was estimated with the jet stream located predominantly south of Yucca Mountain, may not represent the absolute glacial maximum for this period.

3

This maximum may have occurred when the jet stream was in transition over Yucca Mountain. Transient events such as the movement of the jet stream cannot, at present, be simulated by the already-computationally-intensive RegCM2 program.

Based on the input from the RegCM2 (i.e., precipitation rates for 64 points on a 50 kilometer spacing over the regional study area), expected net infiltration rates for the Yucca Mountain area were calculated by Flint and Hevesi (written communication, 1997) of the USGS using a three-step process. The relationship between precipitation and net infiltration is non-linear because net infiltration is a function of the soil storage capacity, evapotranspiration, runoff and other factors including the amount and timing of precipitation. The first step of the process is to determine the ratio of future or past infiltration to present-day infiltration at each grid point, and to interpolate over the regional study area to determine the change in precipitation (precipitation increased 17% for the 2x CO_2 scenario and 71% for the 21-ka pluvial scenario). Second, the kriged changes in precipitation are combined with a present-day precipitation map to create new maps defining precipitation for the two scenarios. Third, the new maps are used in combination with the Maxey-Eakin method to determine net recharge. The Maxey-Eakin method divides basin areas into infiltration zones that are classified based on the percentage of the average annual precipitation within the zone that will become net infiltration (Flint et al., 1996). Present-day infiltration rates were estimated by the USGS using a numerical water balance model (Flint et al., 1996). For the 2x CO_2 scenario, the model domain was classified as one Maxey-Eakin infiltration zone, and net infiltration rates increased throughout the model domain by a factor of two. For the 21-ka pluvial

scenario, the Maxey-Eakin method was applied to smaller infiltration zones rather than the entire model domain, and a more realistic, spatially varying increase in net infiltration was estimated.

2.2 Conceptual Model and Model Parameters

An overview of the geological and hydrological characteristics of the Yucca Mountain site is presented in the first paper of this special issue entitled "Overview of Scientific Investigations at Yucca Mountain - The Potential Repository for High-Level Nuclear Waste" by Bodvarsson et al. This paper describes the conceptual model of the UZ flow system which was used for development of the 3-D UZ flow model. The first conceptual model of the UZ at Yucca Mountain, developed by Montazer and Wilson (1984), has subsequently been updated (Hoxie, 1989; Bodvarsson et al., 1996; Rousseau et al., 1996; Bodvarsson and Bandurraga, 1997) based on an increasing understanding of the hydrologic system and new data from field and laboratory studies.

2.2.1 Model Parameters

Modeling was conducted using a layer-averaged property set previously calibrated (Bandurraga, 1996; Wu et al., 1996; Bandurraga et al., 1997) through an inverse modeling process that involved matching saturation and water potential profiles in individual boreholes against measured data using ITOUGH2 (Finsterle, 1993), a parameter estimation code. The model was also compared with available temperature,

pneumatic, and geochemical data (Wu et al., 1996), and perched water data (Wu et al., 1997). Thermal properties, including wet and dry thermal conductivity, rock grain density and rock grain specific heat (Francis; 1997) were used in conjunction with the model parameter set developed by Bandurraga et al. (1997).

2.2.2 Perched Water

Calibration of the 3-D, UZ site-scale model using perched water data was conducted and described in a separate report (Wu et al., 1997), and the resulting parameter set is used for this paper.

2.3 Study Area Discretization

The 3-D, UZ, site-scale model grid was developed by first creating a horizontal two-dimensional (2-D) grid, and then using isopach maps of hydrogeologic units to vertically discretize the study area from the ground-surface to the water table (Wittwer et al., 1992; Haukwa and Chen, 1996; Haukwa and Wu, 1997). The horizontal grid and boundaries (Figure 1) were chosen based on geologic and hydrologic information at the site, including the location of faults, key hydrologic features, and the location of borehole data and modeling objectives (Wittwer et al., 1995, Haukwa and Chen; 1996, Haukwa and Wu, 1997). Horizontal boundaries were chosen to ensure that critical features and data are captured, and that the boundaries do not interfere with flow patterns within the proposed repository area.

The horizontal boundaries are modeled as no-flux boundary conditions (the default condition for TOUGH2). Both the top boundary, which represents the ground surface or the bottom of surficial alluvium deposits, and the bottom boundary, which represents the water table, are treated as Dirichlet boundaries (constant, but distributed, gas pressures and constant liquid saturations). The water table is assumed to be a flat, stable surface at an elevation of 730 m. Gas pressure conditions at each bottom boundary are estimated relative to an observed gas pressure value of 0.92 bars at an elevation of 730 meters (Ahlers et al., 1995 and Ahlers et al., 1995a). Surface gas pressure of the system was determined by running TOUGH2 to steady-state using constant temperature (25 °C), specified bottom gas pressure, and applied surface net infiltration conditions. For the non-isothermal simulations, temperature is specified at the top and bottom boundaries, and gas pressure at the surface is allowed to vary. Future climatic conditions may increase the elevation of the water table by as much as 120 meters or more (Czarnecki, 1984); however, the impact of these changes is not considered in this paper.

Thermo-physical properties of liquid water and vapor are internally generated in the TOUGH2 code within experimental accuracy from steam table equations (International Formulation Committee, 1967). Air is treated as an ideal gas, and the additivity of partial pressures is assumed for air/vapor mixtures.

The spatial distribution of net infiltration along the top ground surface boundary was recently estimated by the USGS using a numerical water balance model (Flint et al., 1996) (Figure 2). Net infiltration estimated using this method ranges from 0 to

approximately 38 mm/yr, and averages 4.9 millimeters/year (mm/yr) distributed over the 3-D model domain. Higher infiltration rates are located in areas of higher precipitation and in areas where little alluvium cover exists to store infiltration and allow evapo-transpiration to occur (Flint et al., 1996). Higher infiltration areas are located near and to the northwest of Borehole USW G-2 and along the north-south ridge of the mountain. Lower infiltration rates are expected at and near the Bow Ridge Fault (the eastern boundary) and in the southwest corner of the model area. Figure 3 shows histograms for the two infiltration maps. Infiltration rates in the 21-ka pluvial scenario are distributed over a wider range of values than the present-day scenario, and no infiltration rate intervals in the 21-ka pluvial scenario contribute more than 0.05 percent of the total flux infiltrating into the mountain.

2.4 Numerical Formulation

Modeling for this study was conducted using TOUGH2, a multiphase, integrated finite difference code developed by Pruess (1991). A key criterion for selecting the numerical formulation appropriate for a highly fractured, heterogeneous system such as Yucca Mountain is the manner in which fracture-matrix interaction is treated. This study uses the generalized effective continuum method (ECM) (Wu et al., 1996), which assumes thermodynamic equilibrium between fracture and matrix at all times. The ECM defines characteristic curves for fracture and matrix flow independently, and adequately models steady-state systems where the equilibrium condition is met (Doughty and Bodvarsson, 1996; Doughty and Bodvarsson, 1997; Wu et al, 1996a).

3. Results

3-D modeling results were analyzed using one-dimensional profiles and 2-D cross sections extracted from TOUGH2 output. The locations of the 2-D cross sections, which show saturation, velocity fields and particle flow paths, are shown in Figure 1. The effect of climate changes on temperature and perched water conditions was also considered.

3.1 2-D Cross Section Analyses

Figures 4 through 6 show saturation contoured along 2-D cross sections extracted from 3-D model results. These figures show the movement of individual particles along a streamline moving through a velocity vector field. The velocity field used is the composite velocity, which combines fracture and matrix velocities, based on the local equilibrium assumption of the ECM. The composite field represents two extreme cases for ground water travel within the system: rapid transport through fractures, and slower movement through the matrix. The actual flow paths and average water travel times may be bracketed based on the fractional mass fluxes of the two fields.

East-West Cross Section C-C', which intersects Borehole USW UZ-14, is depicted in Figure 4. This figure shows the results of the present-day scenario. Also illustrated in Figure 4 are saturation contours, particle flow paths and the observed location of perched water. Some lateral diversion occurs above the PTn hydrogeologic unit due to a capillary barrier effect, and above the perched water zones due to a permeability barrier effect.

9

Lateral diversion above the PTn due to a capillary barrier effect was first hypothesized by Montazer and Wilson (1984), who stated that water in the unsaturated zone at Yucca Mountain could not flow from a material with relatively fine grains or fractures to a material with relatively coarse grains or fractures until the differences between the capillary rise of the two layers is exceeded. Capillary barriers are a function of the saturated hydraulic conductivity, the angle of the interface between units, the percolation rate and the air-entry pressure of the media (Ross, 1990, Flint, 1996). In order for this phenomenon to occur above the PTn hydrologeologic unit, an abrupt and extensive discontinuity is necessary (Bodvarsson and Bandurraga, eds., 1996). Due to local heterogeneities at the interface, gradational transitions and local heterogenity in the properties of each layer, extensive lateral diversion may not be observed at the interface between the TCw and PTn hydrogeologic units. A detailed discussion of the conditions necessary for a capillary barrier effect to occur at Yucca Mountain is discussed in Flint (1996). Numerical modeling of capillary barriers is discussed by Oldenburg and Pruess (1993).

Lateral diversion above the CHn hydrogeologic unit (or the basal vitrophyre of the TSw hydrogeologic unit) due to a permeability barrier. Permeability barriers, which may occur when vertical fluxes are greater than the saturated hydraulic conductivities, are a function of the saturated hydraulic conductivities, the flux rate, and the angle of interface between materials. Field evidence, which suggests that lateral diversion may occur below the repository horizon, includes perched water occurrences, the low permeabilities of

altered zeolitic units, percolation fluxes estimated from temperature profiles, and some geochemical observations (Bodvarsson and Bandurraga, eds., 1996).

Figures 5 and 6 show the results of the future climate scenario simulations along Cross Section C-C'. As infiltration increases, saturations and the volume of the perched water body increase and the time required for an individual particle to travel from the surface to the water table through an individual velocity vector field decreases. Figures 5 and 6 also show a decrease in the lateral diversion of water along the PTn hydrogeologic unit (represented without fractures) and an increase in the lateral diversion above zeolitic layers within the CHn hydrogeologic unit. Above the PTn hydrogeologic unit, lateral diversion at Borehole USW UZ-14 decreases from approximately 500 meters in the present-day scenario to approximately 250 meters in the 21-ka pluvial scenario. Below the repository horizon, lateral diversion increases from less than 200 meters in the present-day scenario to almost 1,500 meters in the 21-ka pluvial scenario. The decrease in lateral diversion along the PTn hydrogeologic unit occurs because as saturation increases, the relative permeability increases and the capillary barrier effect decreases, reducing the capability of this layer to divert moisture. The inverse relationship between percolation flux and lateral flow was also seen by Wu et al., 1996 and Wilson, 1996. This The zeolitic layers within the CHn hydrogeologic unit, however, show the opposite effect. This result occurs because as percolation flux exceeds the saturated hydraulic conductivities of these layers, any additional water is laterally diverted.

Results of the present-day, the 2x CO_2 and the 21-ka pluvial scenarios along North-South

Cross Section A-A' are displayed in Figures 7 through 9. Similar to Cross Section C-C',

these figures show increased saturation and decreased travel times due to increased

infiltration. Travel time to the perched water zone in Borehole USW UZ-14 is less along

the north-south cross section than along the east-west cross section because due to the 3-

D nature of the velocity components, movement of a particle along a flow path may vary

depending on the direction selected for a 2-D cross section. North-South Cross Section

A-A' shows southward lateral redistribution of moisture above the perched water body at

Borehole USW G-2 south toward Borehole USW UZ-14. This movement follows the dip

of the beds. Lateral diversion along the CHn hydrogeologic unit also increases along the

north-south cross section as infiltration increases and the percolation capacity is

exceeded. Southward diversion increases at Borehole USW G-2 from over 800 meters in

the present-day scenario to over 1,200 meters in the 21-ka pluvial scenario.

3.2 Effect on Saturations

Figure 10 shows changes in saturation due to changes in climatic conditions at Borehole

USW SD-12, located within the potential repository boundary. Normal refers to the

present-day scenario (Flint et al., 1996), 2x refers to the 2x CO_2 scenario, and 21-ka refers

to the 21-ka pluvial scenario. The location of the borehole is shown in Figure 1.

Changing climatic conditions has little overall impact on saturations which are primarily

controlled by the material type and corresponding rock properties. Changes in saturation

are most noticeable within the highly fractured TSw hydrogeologic unit. Here, increased

12

infiltration increases the extent of the perched water zone, where wet core was recovered overlying a zone where geologic units of decreased fracture and/or matrix permeability exist (in this case, the basal vitrophyre of TSw hydrogeologic unit). The model also simulates fully or nearly saturated conditions above the zeolitic layer at the middle of the CHn hydrogeologic unit, suggesting that perched water may also form at this location. Other boreholes where the model indicated near or fully saturated conditions include USW SD-7, USW SD-9 and USW UZ-14.

3.3 Potential Rise of Perched Water

Changes in the elevation of the perched water bodies varied from 0.1 m to 4.9 m for the 2x CO_2 scenario and from 0.2 to 7.9 m for the 21-ka pluvial scenario. The smallest changes are found in Boreholes USW UZ-14 and USW G-2, because additional water is laterally diverted away from these boreholes. The largest change occurred at USW SD-12, where water perches above the basal vitrophyre of the TSw hydrogeologic unit (Rousseau et al., 1996) and increased infiltration increased the elevation of the perched water body by 4.9 m for the 2x CO_2 scenario, and by 7.9 m for the 21-ka pluvial scenario. This increase occurs because water that is infiltrating from nearby higher infiltration zones is diverted laterally and concentrates at Borehole USW SD-12, where the Ghost Dance fault acts as a barrier to further lateral flow. A large increase is also observed at the isolated perched water body at Borehole USW SD-7, where perching occurs above the altered, zeolitic layers within the CHn hydrogeologic unit, and lateral flow may be also blocked by the Ghost Dance Fault (Striffler, 1996).

3.4 Effect on Percolation Flux at the Repository Horizon

The quantity and spatial distribution of percolation at the repository horizon is a key factor that can affect seepage into drifts, the corrosion environment surrounding buried waste canisters, radionuclide migration, and a variety of other factors. Because percolation flux is difficult to measure directly, numerical models play an important role in percolation flux estimation, particularly under perturbations such as increased infiltration. Figures 11 and 12 show 3-D, perspective views of total (fracture and matrix) saturation at the repository horizon for the present-day and 2x CO_2 scenario. Increased infiltration increases percolation flux, but does not appear to significantly affect the spatial distribution of regions of relatively high or low percolation flux at the repository horizon. This occurs because, as shown in 2-D cross sections, above the repository horizon lateral diversion is small, and increased infiltration promotes vertical flow. The most significant changes occur in the northwest portion of the model, and in the vicinity of the proposed repository between the Solitario Canyon and Ghost Dance Faults.

3.5 Effects on Temperature

The effect of climatic changes on temperature was investigated using a calibrated parameter set and a transient, non-isothermal simulation. The transient pulse was imposed on a steady-state flow field. Figure 13 shows a comparison of observed and simulated temperature profiles at Borehole USW SD-12. No effect on the temperature profile is observed after 1,000 years of increased infiltration because the percolation flux

is too small to impact temperature. After 10,000 years, however, increased infiltration increases convective forces that cool groundwater, causing a reduction in temperature. There is little difference between temperature profiles at the larger times because the system has reached steady state.

4. Summary and Conclusions

The calibrated 3-D UZ site-scale model provides an opportunity to examine how climate change may affect the movement and distribution of moisture within the UZ at Yucca Mountain. This is critical to understanding ambient conditions as well as to understanding the environment that may surround the emplaced waste throughout the potential lifespan of the repository.

Simulations of future climatic conditions using the 3-D UZ site-scale model increased elevations of existing perched water bodies. Changes in elevation of the perched water bodies varied from approximately 0 to 8 meters. Increased infiltration decreased lateral diversion above the PTn hydrogeologic unit (represented without fractures) from 500 to 250 meters, and increased diversion above low-permeability layers below the repository horizon from 400 to 1300 meters. The decrease in lateral diversion along the PTn hydrogeologic unit occurs because as saturation increases, the relative permeability increases and the capillary barrier effect decreases, reducing the capability of this layer to divert moisture. This result reflects LBNL's 1996 parameter set in the PTn hydrogeologic unit (i.e., no fractures) (Bodvarsson and Bandurraga, eds.), which has

since been updated to include fractures within the PTn (Bodvarsson et al., eds., 1997). Within the CHn hydrogeologic unit, the zeolitic layers have very low permeabilities, and as a result, increased saturation forces the lateral diversion of additional water. Because these zeolitic layers have a high capability of retarding radionuclides, determination of the path from the repository horizon to the water table is a key factor in estimating potential concentrations at the accessible environment. Increased infiltration increases percolation flux, but does not appear to significantly affect the spatial distribution of regions of relatively high or low percolation flux at the repository horizon. This occurs because, above the repository horizon, lateral diversion is small, and increased infiltration promotes vertical flow. The most significant changes occur in the northwest portion of the model and between the Solitario Canyon and Ghost Dance Faults. Analysis and collection of additional geologic, hydrogeologic, and geochemical data will decrease uncertainty in the role of the PTn and altered CHn hydrogeologic units in creating barriers to vertical flow, and improve confidence in future climatic predictions.

References

Ahlers, C.F.; Bandurraga, T.M.; Bodvarsson, G.S.; Chen, G.; Finsterle, S.; and Wu, Y.S. 1995. Summary of Model Calibration and Sensitivity Studies Using the LBNL/USGS Three-Dimensional Unsaturated-Zone Site-Scale Model. Yucca Mountain Project Milestone 3GLM107M, Lawrence Berkeley National Laboratory, Berkeley, CA.

Ahlers, C.F.; Bandurraga, T.M.; Bodvarsson, G.S.; Chen, G.; Finsterle, S.; and Wu, Y.S. 1995a. Performance Analysis of the LBNL/USGS Three-Dimensional Unsaturated-Zone Site-Scale Model. Yucca Mountain Project Milestone 3GLM105M, Lawrence Berkeley National Laboratory, Berkeley, CA.

Bandurraga, T.M. 1996. "Geological Model Development and Vertical Layering Scheme for the Numerical Grid." Chapter 2 of Development and Calibration of the Three-Dimensional Site-Scale Unsaturated-Zone Model of Yucca Mountain, Nevada, edited by G.S. Bodvarsson and M. Bandurraga. Yucca Mountain Site Characterization Project Milestone OBO2, Report LBNL-39315, Lawrence Berkeley National Laboratory, Berkeley, CA.

Bandurraga, T.M.; Wu, Y.S.; Ritcey, A.C.; Sonnenthal, E.; Ahlers, C.F.; Haukwa, C.; and Bodvarsson, G.S. 1997. UZ Site-Scale Model Calibration, FY97. Lawrence Berkeley National Laboratory Level 4 Milestone SP924UDM4, Yucca Mountain Site Characterization Report, Lawrence Berkeley National Laboratory, Berkeley, CA.

Bodvarsson, G.S., T.M. Bandurraga, and Y.S. Wu, 1996. "Development of the Unsaturated Zone Model in Fiscal Year 1996." Chapter 1 of Development and Calibration of the Three-Dimensional Site-Scale Unsaturated-Zone Model of Yucca Mountain, Nevada, edited by G. S. Bodvarsson and T. M. Bandurraga. Yucca Mountain Site Characterization Project Milestone OBO2, Report LBNL-39315 Lawrence Berkeley National Laboratory, Berkeley, CA:

Bodvarsson, G.S. and T.M. Bandurraga, eds., 1996. "Development and calibration of the 3-D site-scale unsaturated-zone model of Yucca Mountain, Nevada", Yucca Mountain Site Characterization Project Report, Lawrence Berkeley National Laboratory, Berkeley, CA, LBNL Report 39315.

Bodvarsson, G.S. and T.M. Bandurraga, 1997. "Conceptual Model of Flow and Transport at Yucca Mountain." Chapter 2 of The Site-Scale Unsaturated Zone Model of Yucca Mountain, Nevada, for the Viability Assessment, edited by G.S. Bodvarsson, T.M. Bandurraga, and Y.S. Wu. Yucca Mountain Project Milestone Report SP24UFM4; LBNL-40376, Lawrence Berkeley National Laboratory,. Berkeley, CA.

Bodvarsson, G.S., T.M. Bandurraga, and Yu-Shu Wu, eds., 1997. "The Site-Scale Unsaturated Zone Model of Yucca Mountain, Nevada, for the Viability Assessment", Yucca Mountain Site Characterization Project Report, LBNL-40376, UC-814, Lawrence Berkeley National Laboratory, Berkeley, CA.

Czarnecki, J.B. 1984. "Simulated effects of increased recharge on the ground-water flow system of Yucca Mountain and vicinity, Nevada-California, Water-Resources Investigations Report, 84-4344, Lakewood, CO.

Doughty, C. and Bodvarsson, G.S. 1996. "Investigation of Conceptual and Numerical Approaches for Evaluating Gas, Moisture, Heat, and Chemical Transport." Chapter 6 of Development and Calibration of the Three-Dimensional Site-Scale Unsaturated-Zone

Model of Yucca Mountain, Nevada, edited by G.S. Bodvarsson and M. Bandurraga, Yucca Mountain Site Characterization Project Milestone OBO2, Lawrence Berkeley National Laboratory, Berkeley, CA.

Doughty, C. and Bodvarsson, G.S. 1997. "Investigation of Conceptual and Numerical Approaches for Evaluating Moisture Flow and Chemical Transport." Chapter 5 of The Site-Scale Unsaturated Zone Model of Yucca Mountain, Nevada, for the Viability Assessment, edited by G.S. Bodvarsson, T.M. Bandurraga, and Y.S. Wu. Yucca Mountain Project Milestone Report SP24UFM4; LBNL-40376, Lawrence Berkeley National Laboratory, Berkeley, CA.

Finsterle S. 1993. ITOUGH2 User's Guide. Version 2.2. Report LBNL-34581, UC-600.: Lawrence Berkeley National Laboratory, Berkeley, CA.

Flint, L.E. 1996. *Characterization of Hydrogeologic Units Using Matrix Properties, Yucca Mountain, Nevada.* U.S. Geol. Surv. Water Resour. Invest. 97-4243. U.S. Geological Survey, Denver, Colorado.

Flint, A. L.; Hevesi, J. A.; and Flint, L.E. 1996. (Unpublished) Conceptual and Numerical Model of Infiltration for the Yucca Mountain Area, Nevada. Milestone Report 3GU1623M, U. S. Geol. Surv. Water Resour. Invest. Rep.: Submitted for publication as a Water-Resources Investigations Report, U.S. Geological Survey, Denver, CO.

Forester, R.M., 1994. "Late glacial to modern climate near Yucca Mountain, NV", from Proceedings of the Fifth Annual International High Level Radioactive Waste Management Conference, Vol 4., pp 2750 -2754.

Francis, N. D., 1997. Memo to Distribution: The base-case thermal properties for the TSPA-VA modeling, SNL, Albuquerque, NM.

Haukwa, C., and G. Chen, 1996. "Grid generation and analysis", Chapter 5 in "Development and calibration of the 3D site-scale unsaturated zone model of Yucca Mountain", Edited by G.S. Bodvarsson and M. Bandurraga, Yucca Mountain Project Milestone Report OB02, Lawrence Berkeley National Laboratory, Berkeley, CA.

Haukwa, C., and Y.S. Wu , 1997. "Grid generation and analysis" in "The site-scale unsaturated zone model of Yucca Mountain, Nevada, for the viability assessment", edited by Bodvarsson, G.S., T.M. Bandurraga, and Y.S. Wu, LBNL Level 3 Milestone, Lawrence Berkeley National Laboratory, Berkeley, CA.

Hoxie, D., 1989. "A conceptual model for the unsaturated-zone hydrogeologic system, Yucca Mountain, Nevada", in Radioactive Waste Management and the Nuclear Fuel Cycle, Vol. 13(1-4) pp. 63-75.

International Formulation Committee, 1967. A formulation of the thermodynamic properties of ordinary water substance, IFC Secretariat, Düsseldorf, Germany.

Jannick, N.O., F. M., Phillips, G. I. Smith and D. Elmore, 1991. A Cl-36 chronology of lacustrine sedimentation in the Pleistocene Owens River system, Geol. Soc. Am. Bull., 103, 1146-1159.

Montazer, P. and W.E. Wilson, 1984. "Conceptual Hydrologic Model of Flow in the Unsaturated Zone, Yucca Mountain, Nevada", USGS WRI Report 84-4345, Lakewood, CO.

Oldensburg, C.M., and Pruess, K., 1993, On numerical modeling of capillary barriers: Water Resources Research, v. 29, no. 4, p. 1045-1056.

Pruess, K., 1991. TOUGH2- A general purpose numerical simulator for multiphase fluid and heat flow, Lawrence Berkeley National Laboratory Report LBL-29400, Lawrence Berkeley National Laboratory, Berkeley, CA.

Ross, Benjamin, 1990. *The diversion capacity of capillary barriers*: Water Resources Research, v. 26, no. 10, p. 2625-2629.

Rousseau, J.E., E.M. Kwicklis, and D.C. Gillies, eds., 1996. Hydrogeology Of The UZ, North Ramp Area Of The Exploratory Studies Facility, Yucca Mountain, Nevada, U.S. Geological Survey Water Resources Investigations Report 96-xxx, U.S. Geological Survey, Denver, Colorado, 267 pp.

Schelling, F.J. and S. L. Thomson, 1997. "Future Climate Modeling Scenarios" SLTR97-0001, Albuquerque, NM.

Smith, G. I., 1984. Paleohydrologic regimes in the southwestern Great Basin 0-3.2 my ago, compared with other long records of "global" climates, Quat. Res., 22, 1-17.

Sonnenthal, E.L., and G.S. Bodvarsson, 1997. "Modeling the Chloride Geochemistry in the Unsaturated Zone", Chapter 15 in "The Site-Scale Unsaturated Zone Model of Yucca Mountain, Nevada, for the Viability Assessment" edited by G.S. Bodvarsson, T.M. Bandurraga and Y.S. Wu, Lawrence Berkeley National Laboratory, Berkeley, CA.

Striffler, Peter, Grady M. O'Brien, Thomas Oliver and Paul Burger, 1996. Perched Water Characteristics and Occurrences, Yucca Mountain, Nevada, USGS Preliminary Report, Denver, CO.

Szabo, B. J., P. T. Kolesar, A. C. Riggs, I. J. Winograd, and K. R. Ludwig, 1994. Paleoclimatic inferences form a 120,000-year calcite record of water-table fluctuation in Browns Room of Devils Hole, Nevada, Quat.Res., 41, 59-69.

Tyler, S. W., J. B. Chapman, S. H. Conrad, D. P. Hammermeister, D.O. Blout, J.J. Miller, M. J. Sully and J. M. Ginanni, 1996. "Soil-water flux in the southern Great Basin, United States: Temporal and spatial variations over the last 120,000 years", Water Resources Research, vol., 32, no. 6, pages 1481-1499.

Wilson, Michael L., 1996. "Lateral Diversion in the PTn Unit: Capillary-Barrier Analysis, in the Seventh Annual International Conference Proceedings from the High Level Radioactive Waste Management Conference, pp. 111-113.

Winograd, I.J., B.J. Szabo, T. B. Coplen, and A. C. Riggs, 1988. A 250,000 year climatic record from Great Basin vein calcite: Implications for the Milankovitch Theory, Science , 242, 1275-1280.

Winograd, I.J., T. B. Coplen, J.M. Landwehr, A. C. Riggs, K.R. Ludwig, B.J. Szabo, P.T. Koesar, and K.M. Revesz, 1992. Continuous 500,000-year climate record from vein calcite in Devils Holes, Nevada, Science, 258, 255-287.

Wittwer, C., G.S. Bodvarsson, M.P. Chornack, A. L. Flint, L.E., Flint, B. D., Lewis, R.W. Spengler, and C.A. Rautman, 1992. Design of a 3-D site-scale model for the unsaturated zone at Yucca Mountain, Nevada, in Proceedings of the Third International Conference on High Level Radioactive Waste Management, American Nuclear Society, La Grange Park, IL, pp. 263-271.

Wittwer, C., G. Chen, G.S. Bodvarsson, M. Chornack, A. Flint, L. Flint, E. Kwicklis, and R. Spengler, 1995. Preliminary development of the LBL/USGS 3-D site-scale model of Yucca Mountain, Nevada, LBL Report LBL-37356, Lawrence Berkeley National Laboratory, Berkeley, CA.

Wu, Y.S., G. Chen, C. Haukwa, and G.S. Bodvarsson, 1996. 3-D model calibration and sensitivity studies, Chapter 8 of Development and calibration of the 3-D site-scale

unsaturated-zone model of Yucca Mountain, Nevada, G.S. Bodvarsson and T. M. Bandurraga, eds., Yucca Project Milestone 0B02, Lawrence Berkeley National Laboratory, Berkeley, CA.

Wu, Y.S.; Ahlers, C.F.; Fraser, P.; Simmons, A.; and Pruess, K. 1996. Software Qualification of Selected TOUGH2 Modules. Report LBNL-39490, UC-800 Lawrence Berkeley National Laboratory, Berkeley, CA.

Wu, Y.S., A. C. Ritcey, E.M. Sonnenthal, T.M. Bandurraga, C. Haukwa, J. P. Fairley, G. Chen, J.H. Li, and G.S. Bodvarsson, 1997. Incorporation of perched water data into the UZ site-scale model, Yucca Project Milestone SP24UCM4, Lawrence Berkeley National Laboratory, Berkeley, CA.

Yang, I. C., G.W. Rattray and Pei Yu, 1996. "Interpretation of chemical and isotopic data from boreholes in the UZ at Yucca Mountain, Nevada" USGS WRI-4085, Denver, CO.
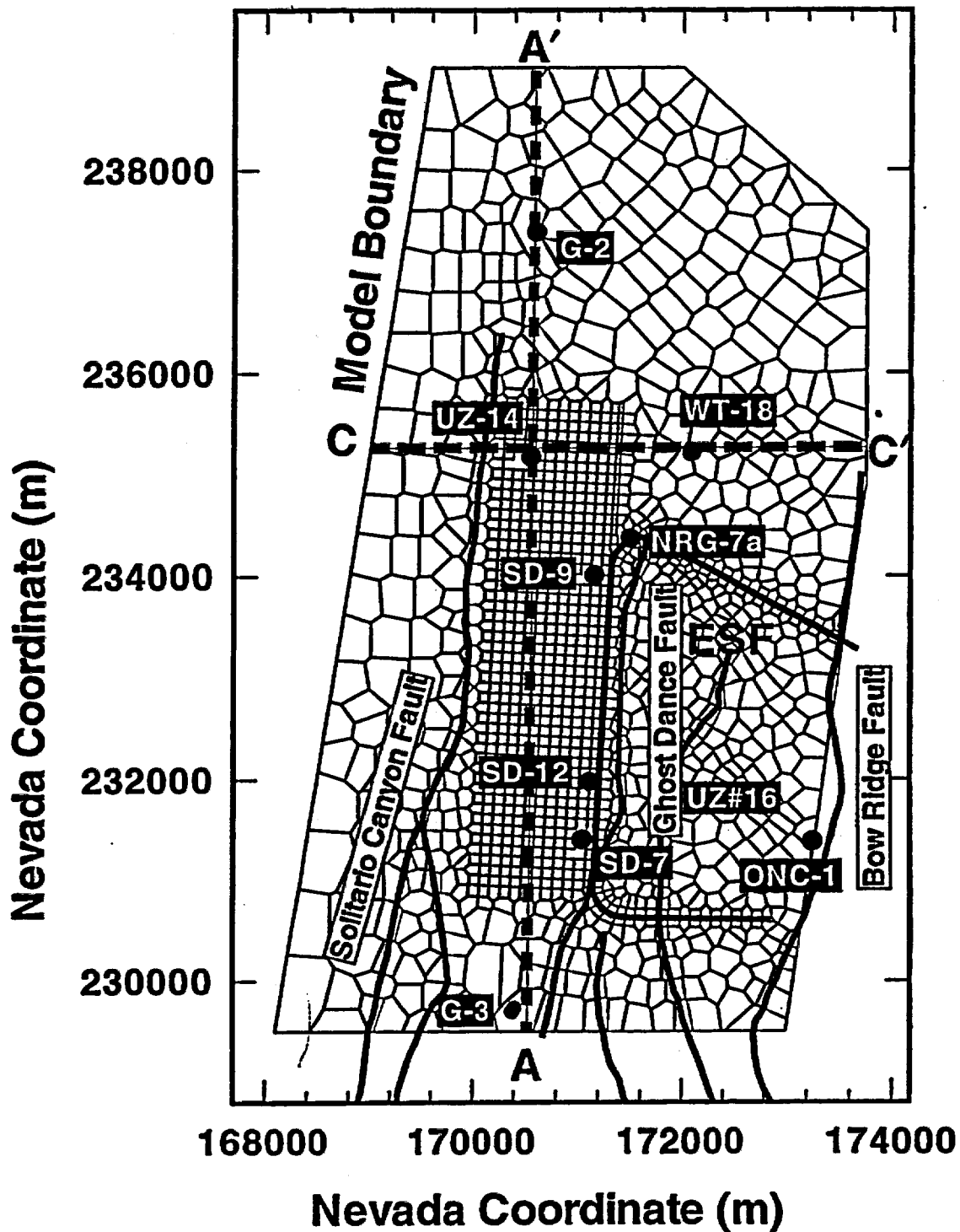
Figure 1: Plan view of the model domain showing boundaries, location of boreholes, faults, cross-sections and the Exploratory Studies Facility (ESF).
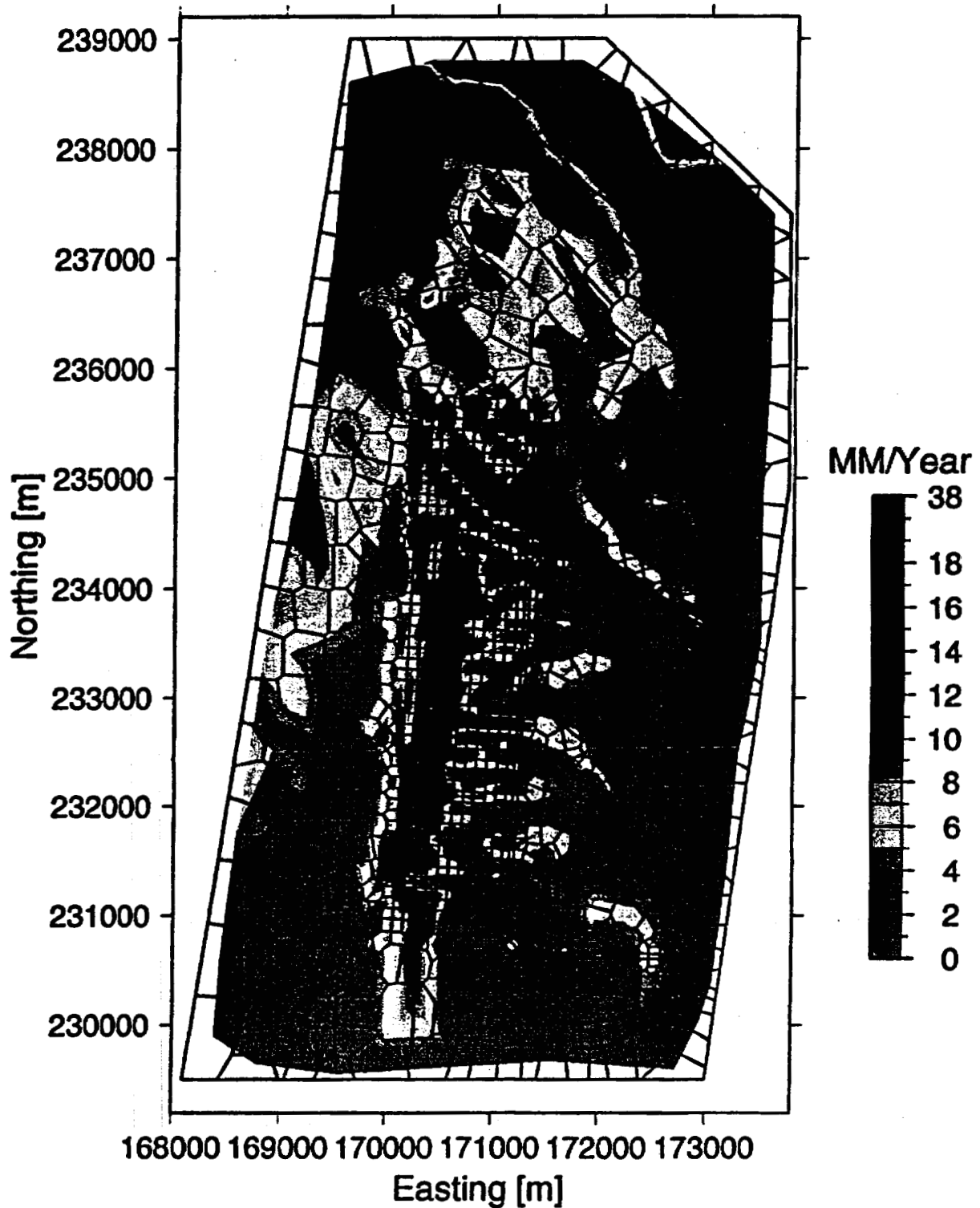
Figure 2: Map showing the spatial distribution of net infiltration rates in mm/yr over the

model domain (from Flint et al., 1996).
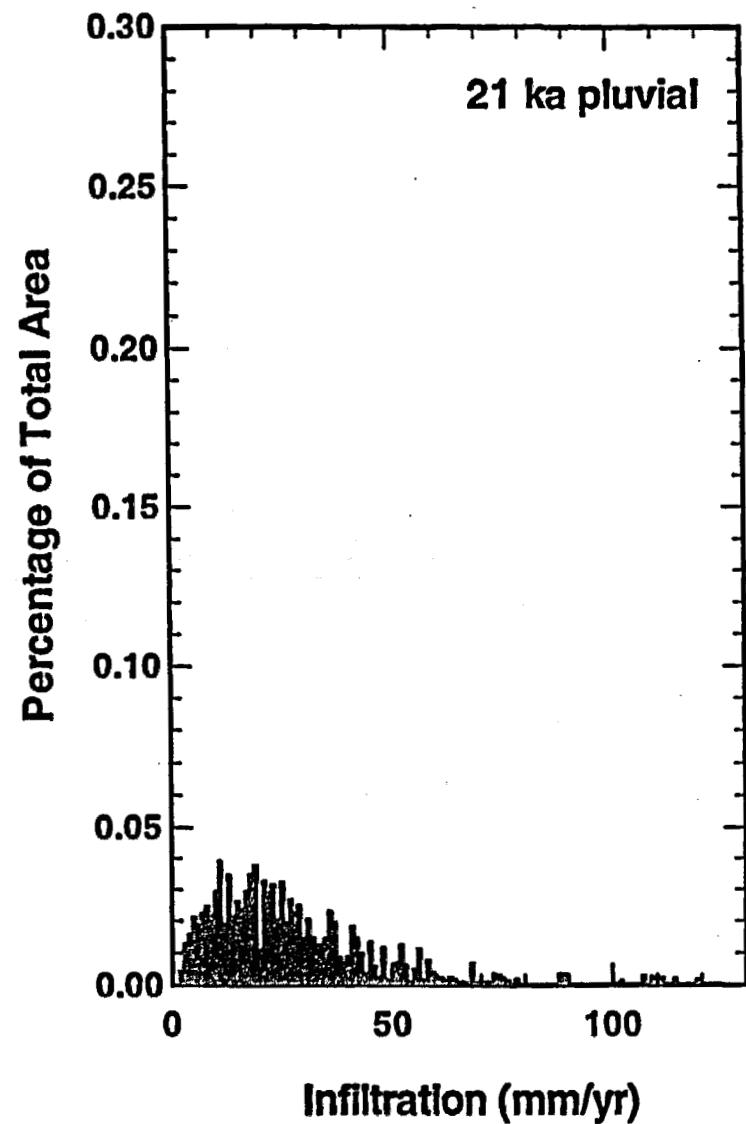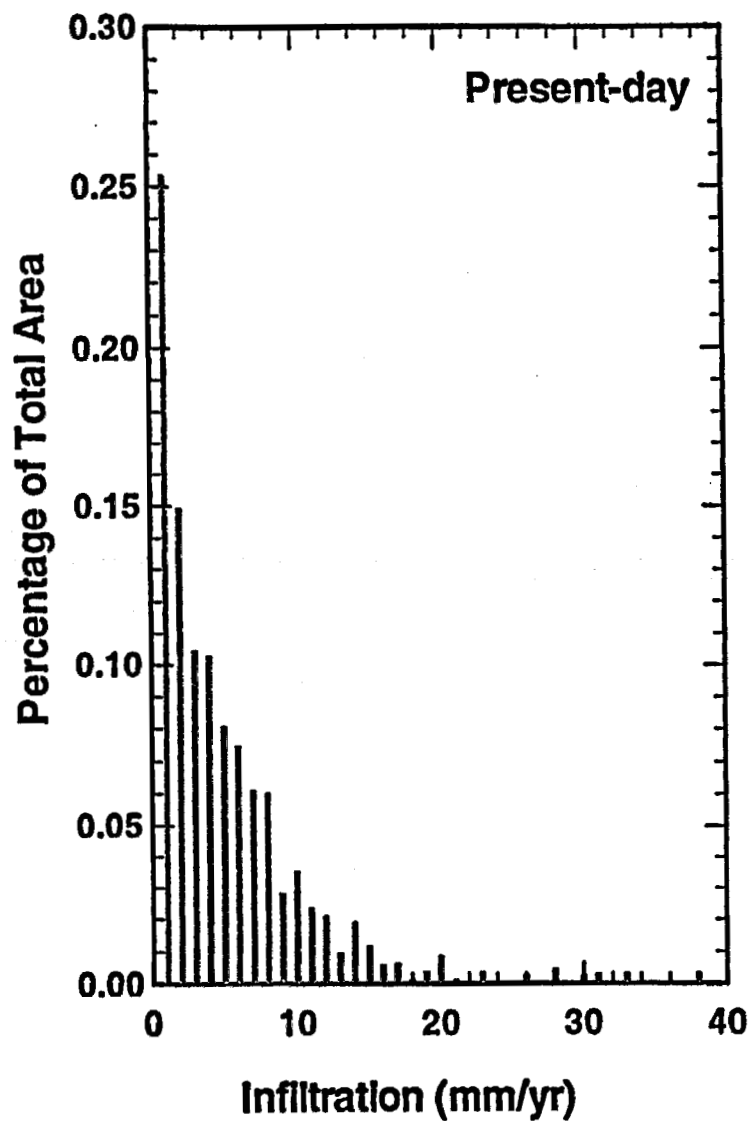
Figure 3: Two histograms showing infiltration (mm/yr) v. percentage of the total area within the model domain for the present-day and 21 ka pluvial scenarios.
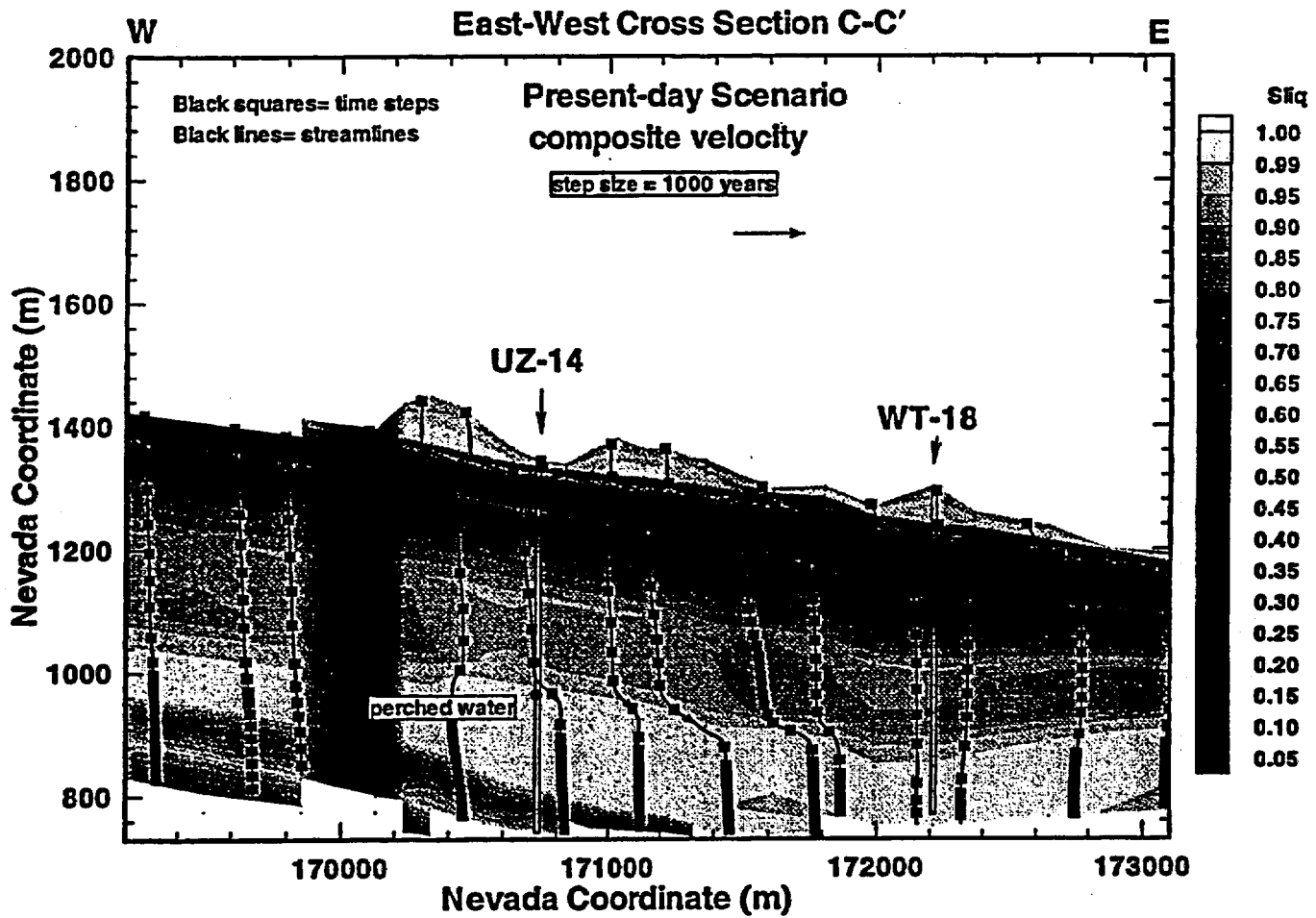
Figure 4: Saturation, velocity field and particle flow paths along
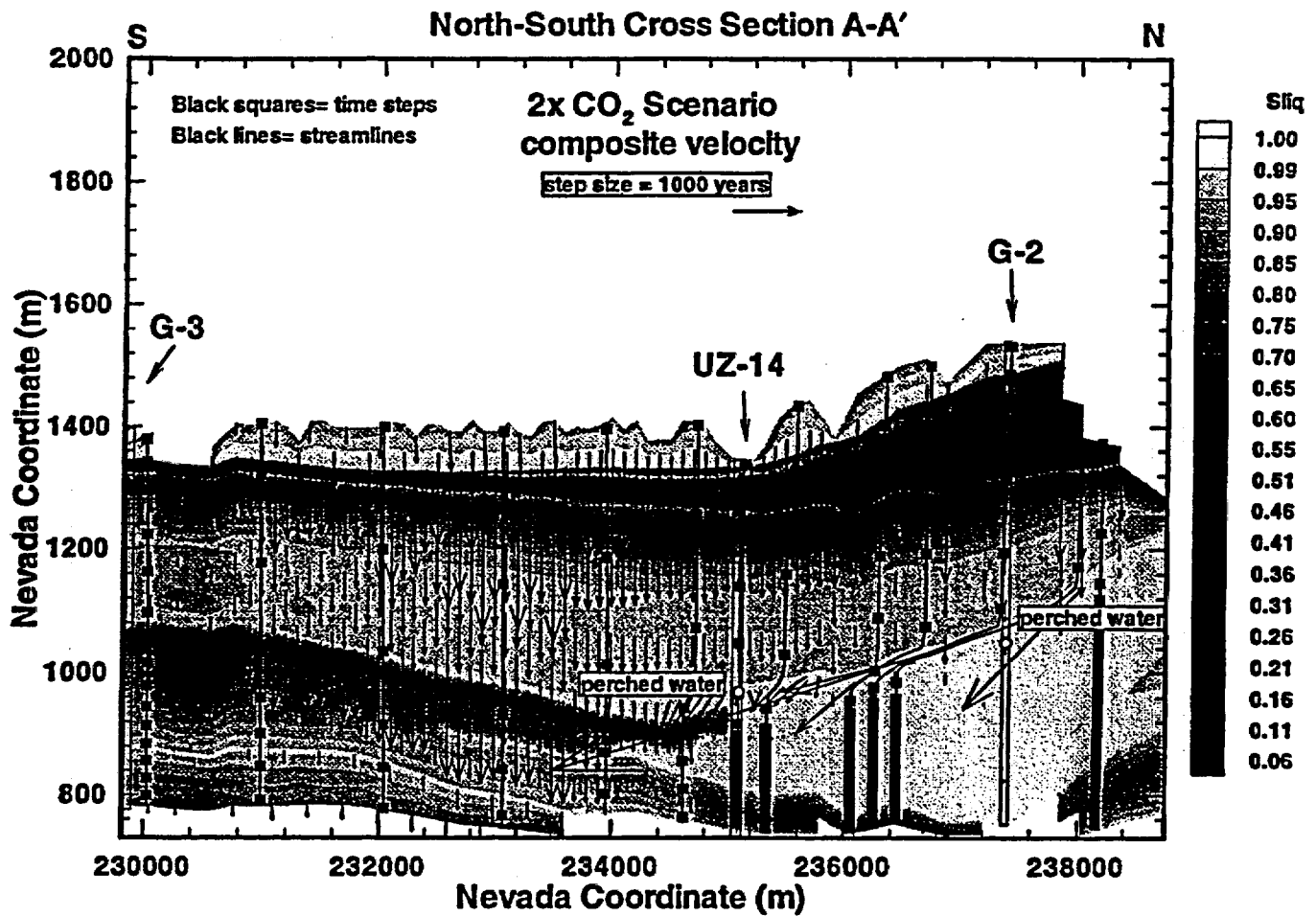East-West Cross Section C-C' (present-day scenario).
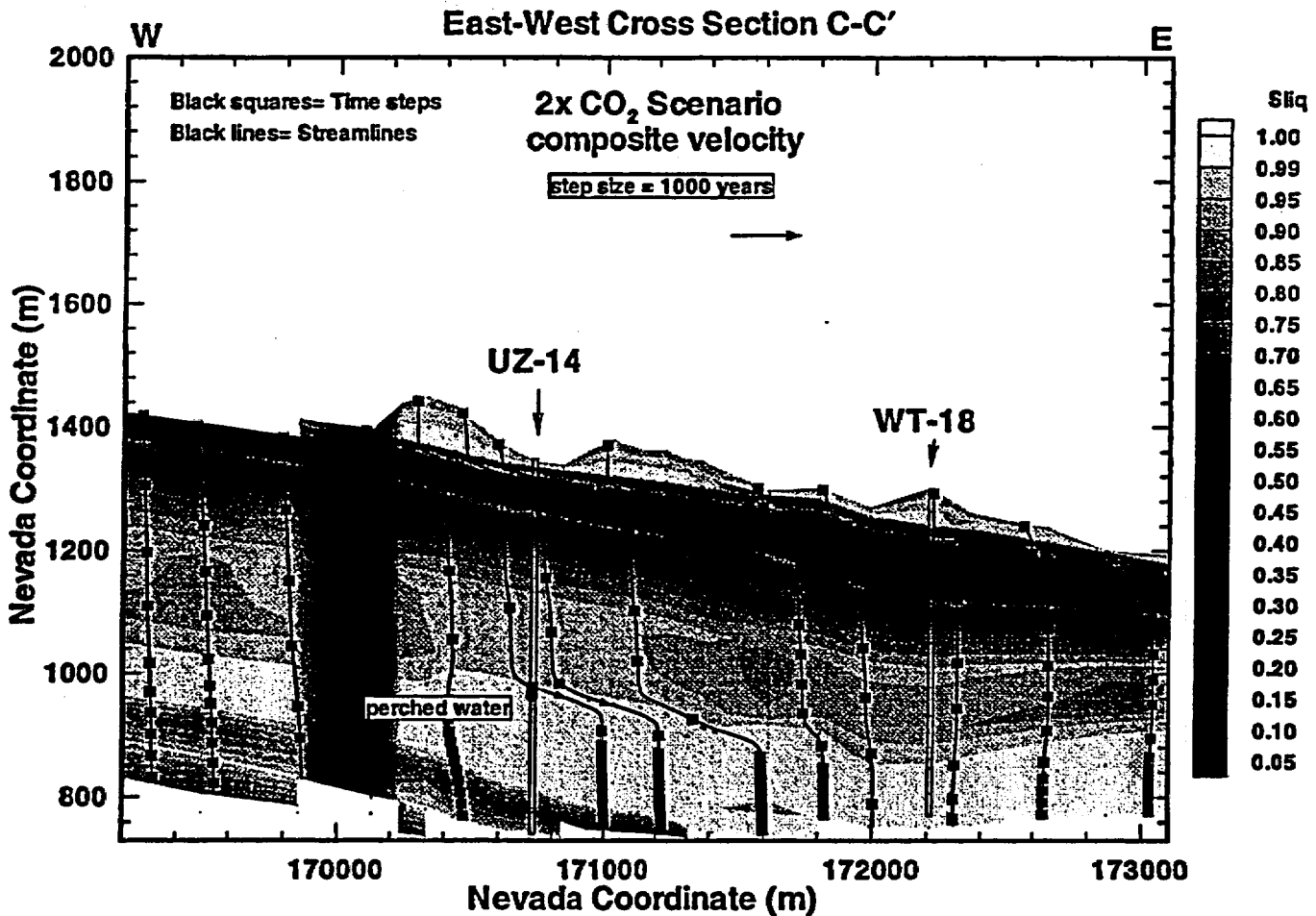
Figure 5: Saturation, velocity field and particle flow paths along East-West Cross Section C-C' (2x CO_2 scenario).
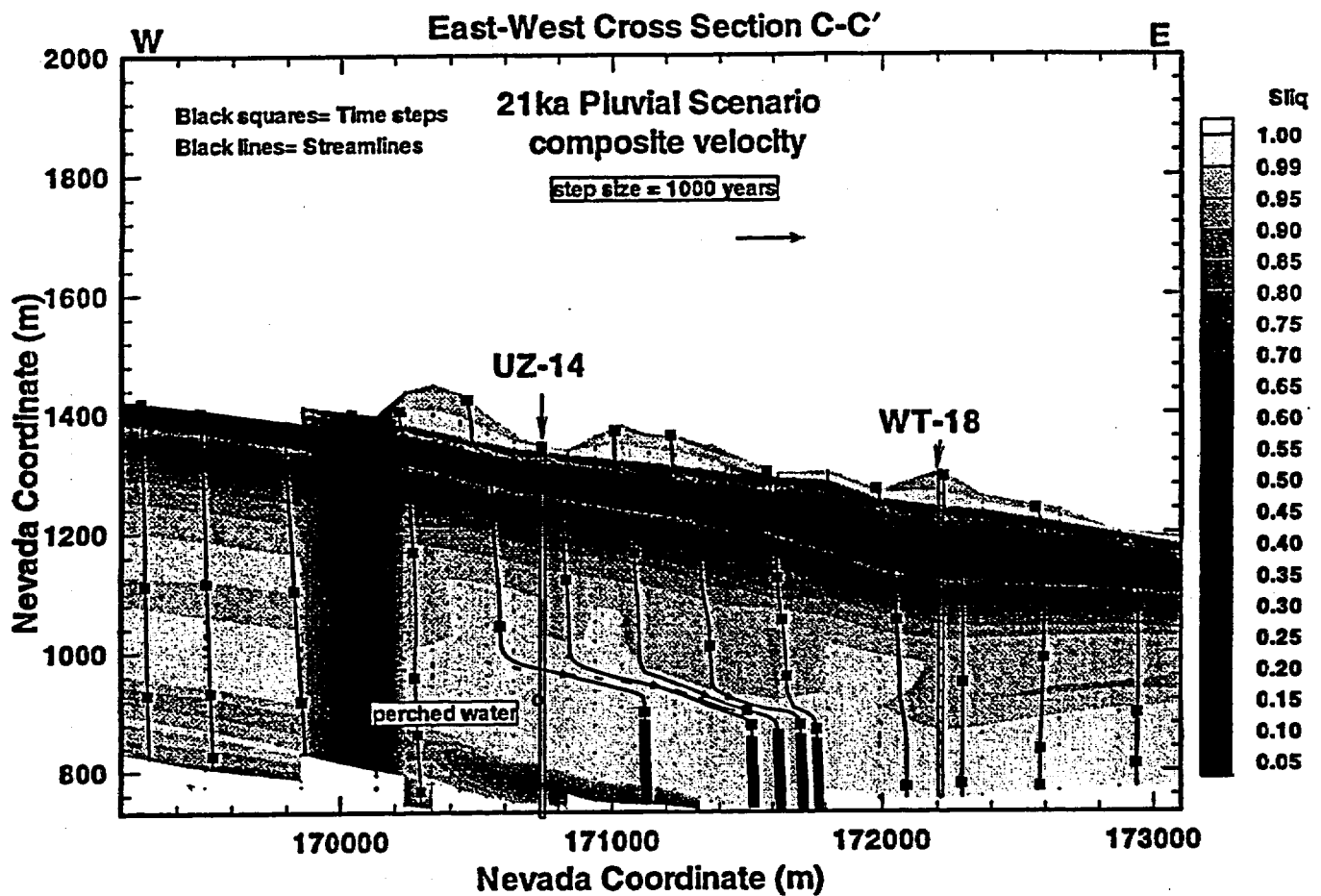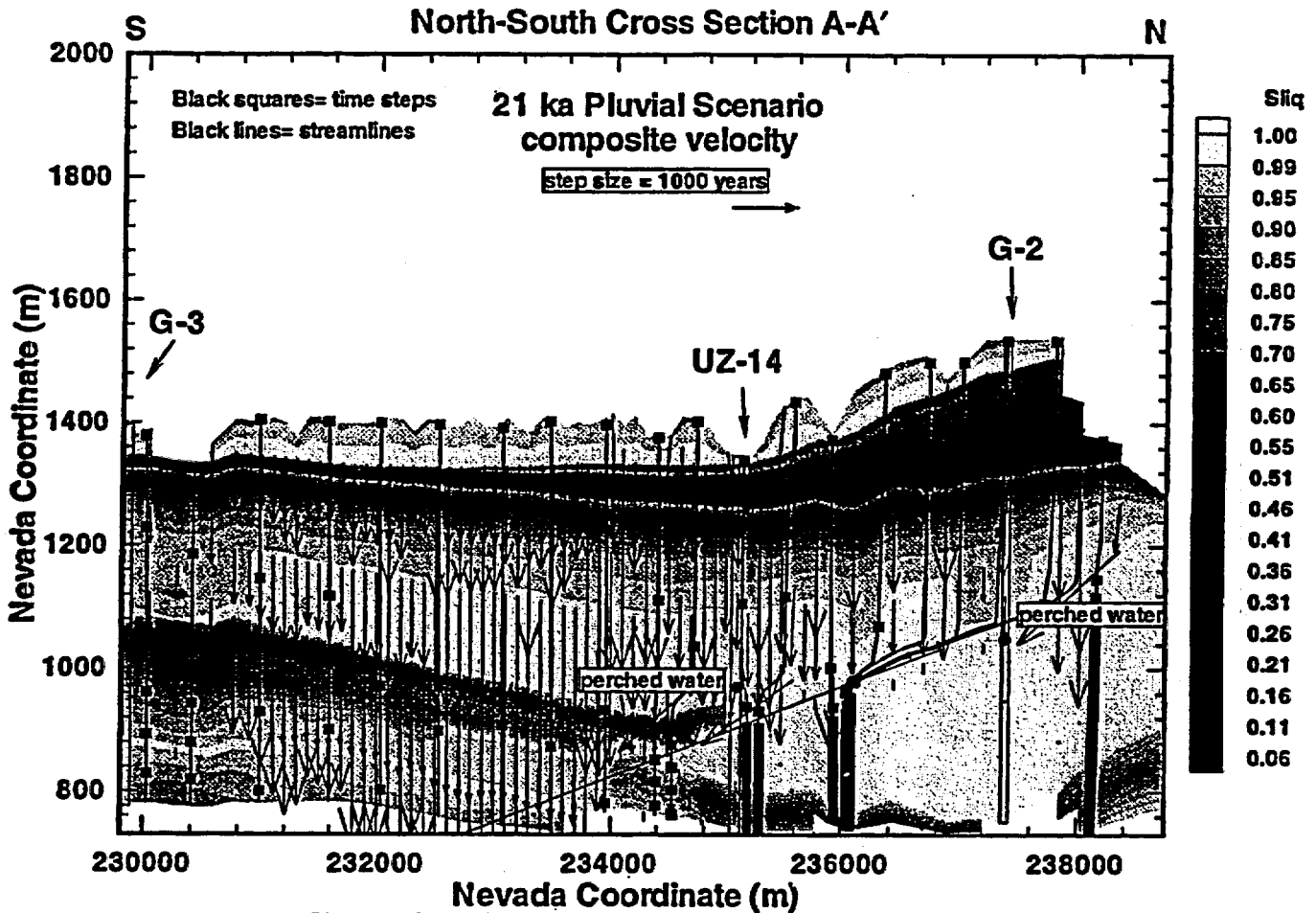
Figure 6: Saturation, velocity field and particle flow paths along
East-West Cross Section C-C' (21 ka pluvial scenario).

North-South Cross Section A-A'

S / N

Present-day Scenario composite velocity

Black squares= time steps
Black lines= streamlines

step size = 1000 years

G-3 / UZ-14 / G-2

perched water

Sliq
1.00
0.99
0.95
0.90
0.85
0.80
0.75
0.70
0.65
0.60
0.55
0.51
0.46
0.41
0.36
0.31
0.26
0.21
0.16
0.11
0.06

Nevada Coordinate (m)
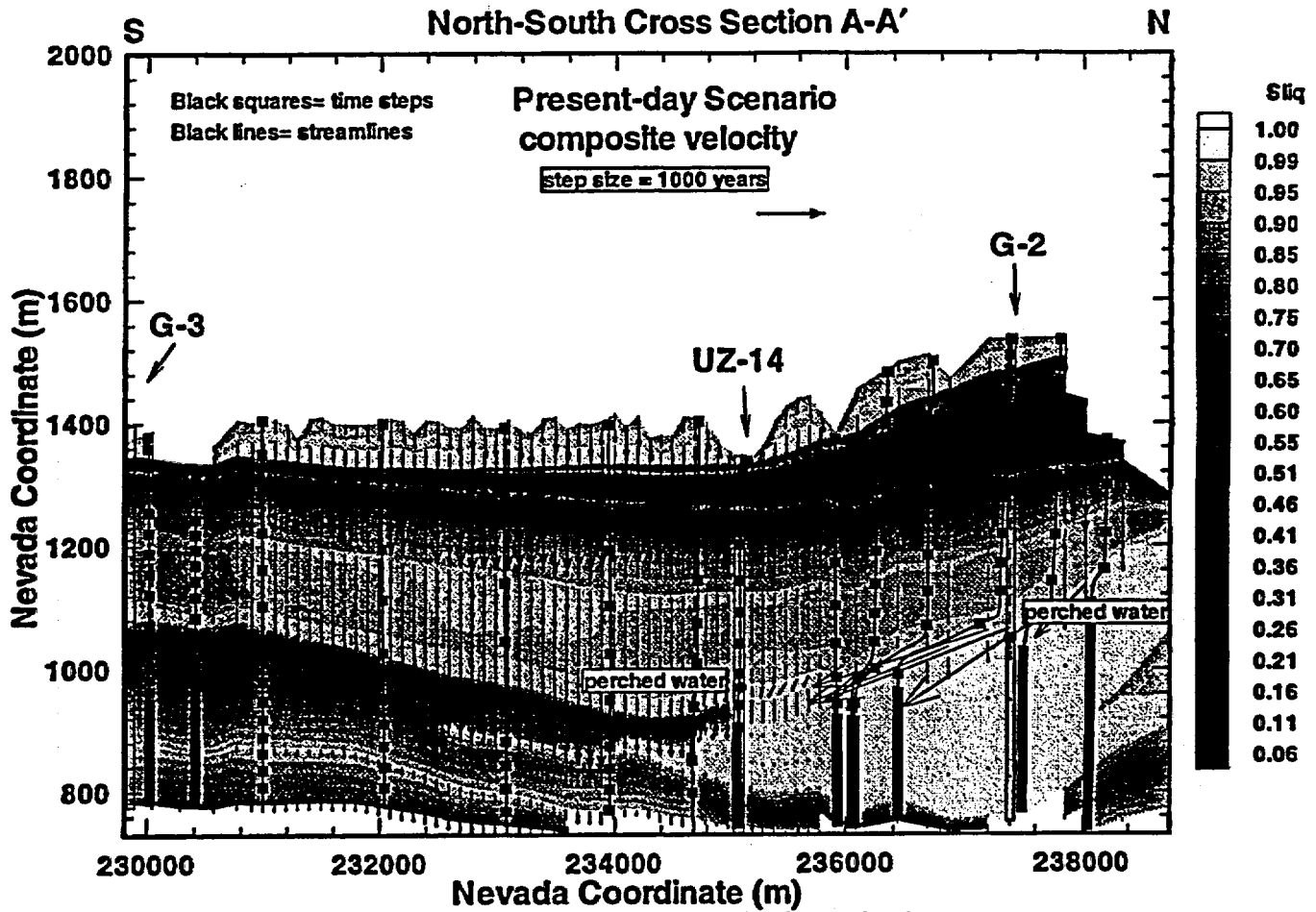
Figure 7: Saturation, velocity field and particle flow paths along
North-South Cross Section A-A' (present-day scenario).

Figure 8: Saturation, velocity field and particle flow paths along
North-South Cross Section A-A' (2x CO_2 scenario).

Figure 9: Saturation, velocity field and particle flow paths along North-South Cross Section A-A' (21 ka pluvial scenario).
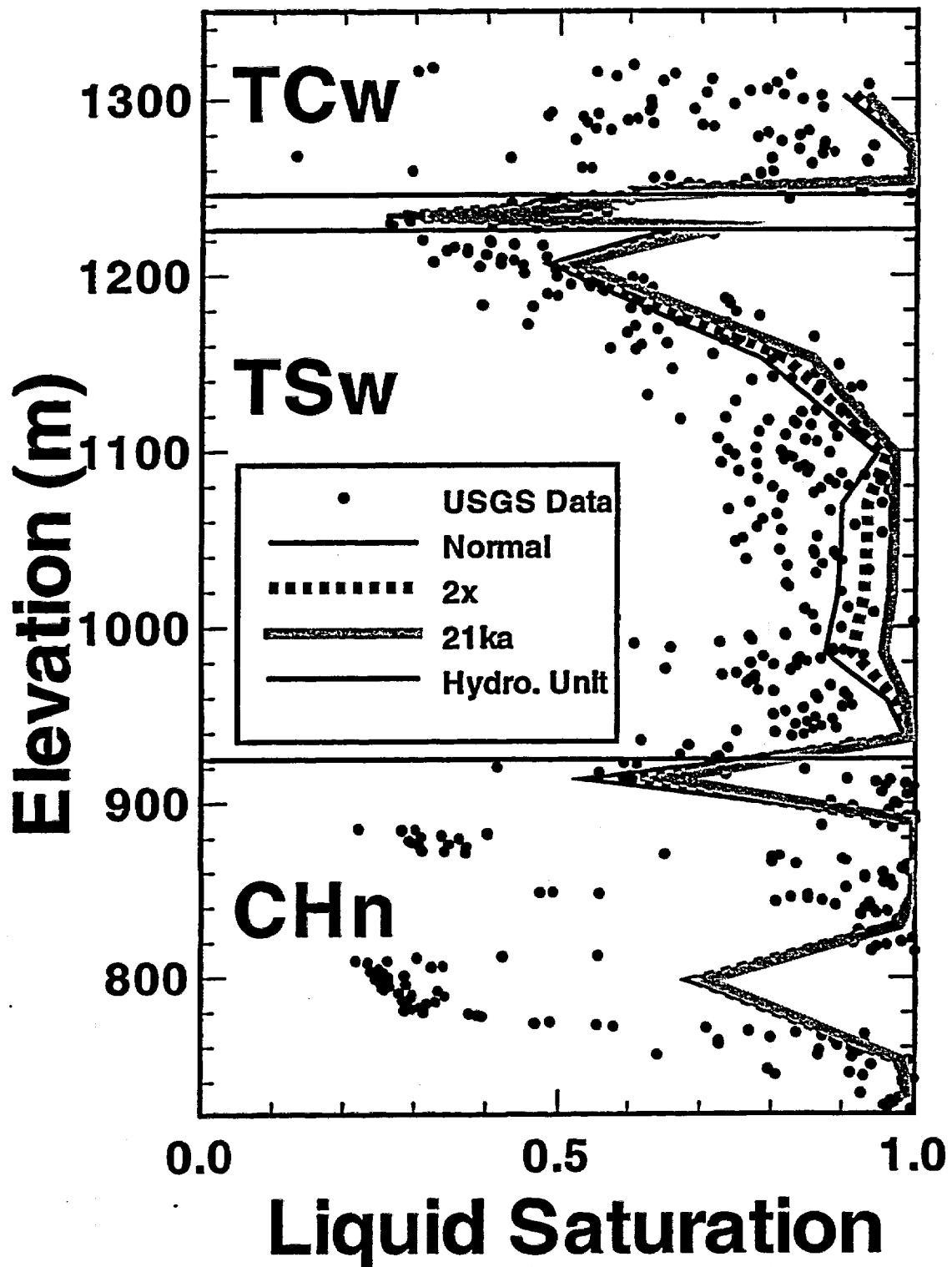
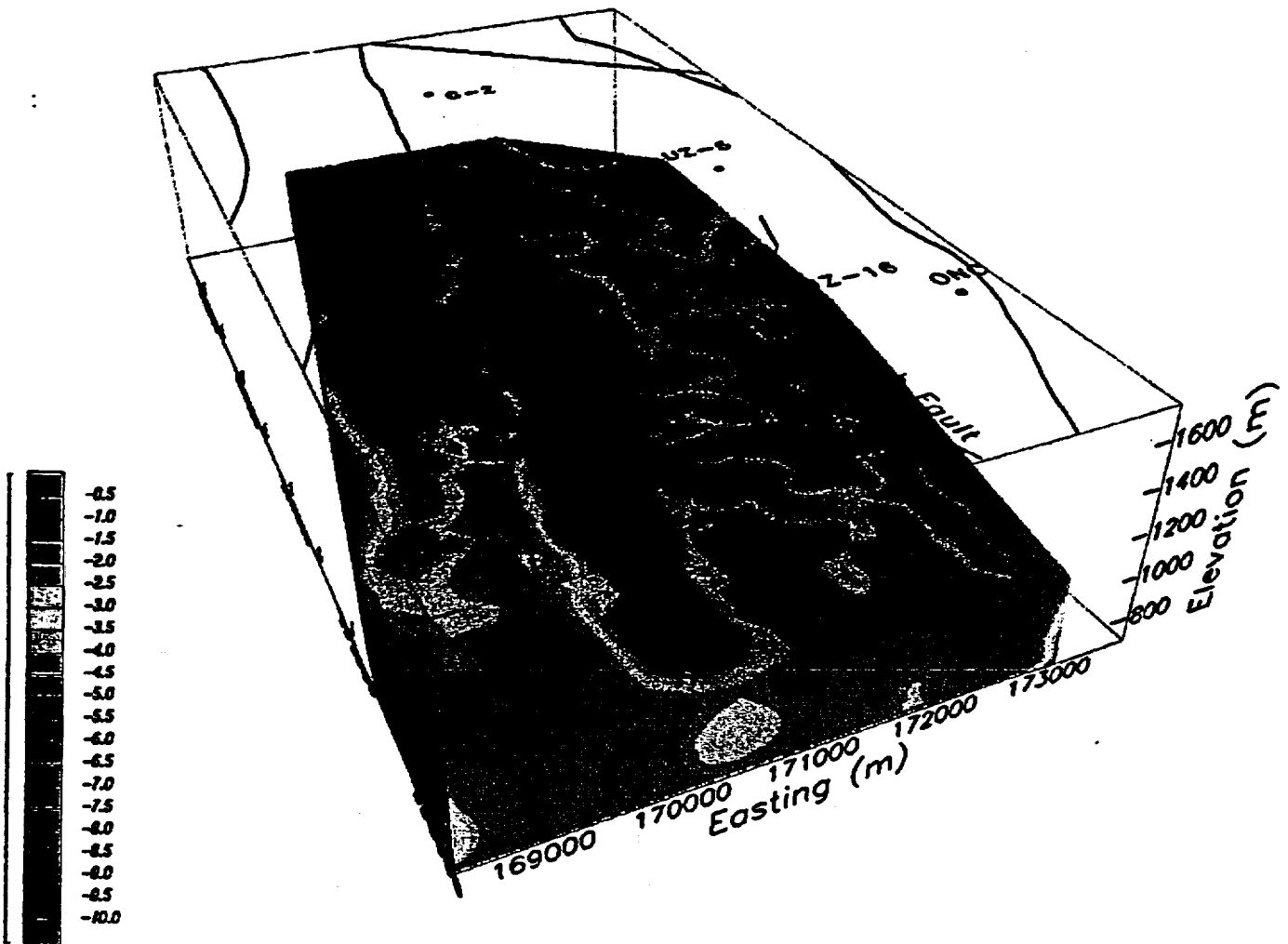Figure 10: Comparison between observed and modeled saturation at borehole USW SD-12.

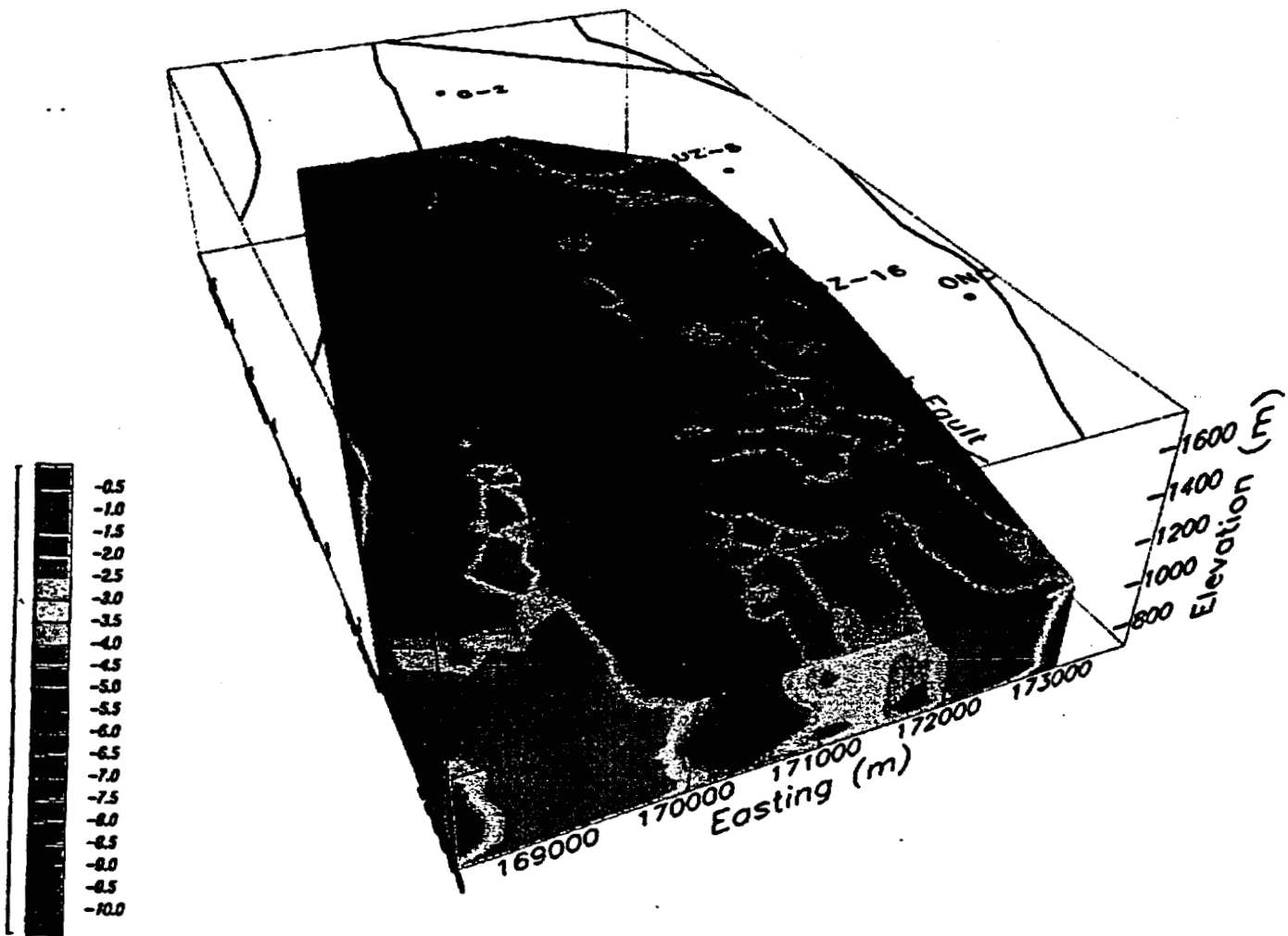Figure 11: A 3-D view of percolation flux in mm/yr at the repository horizon (present-day scenario).

Figure 12: A 3-D view of percolation flux in mm/yr at the repository horizon (2 x CO_2 scenario).
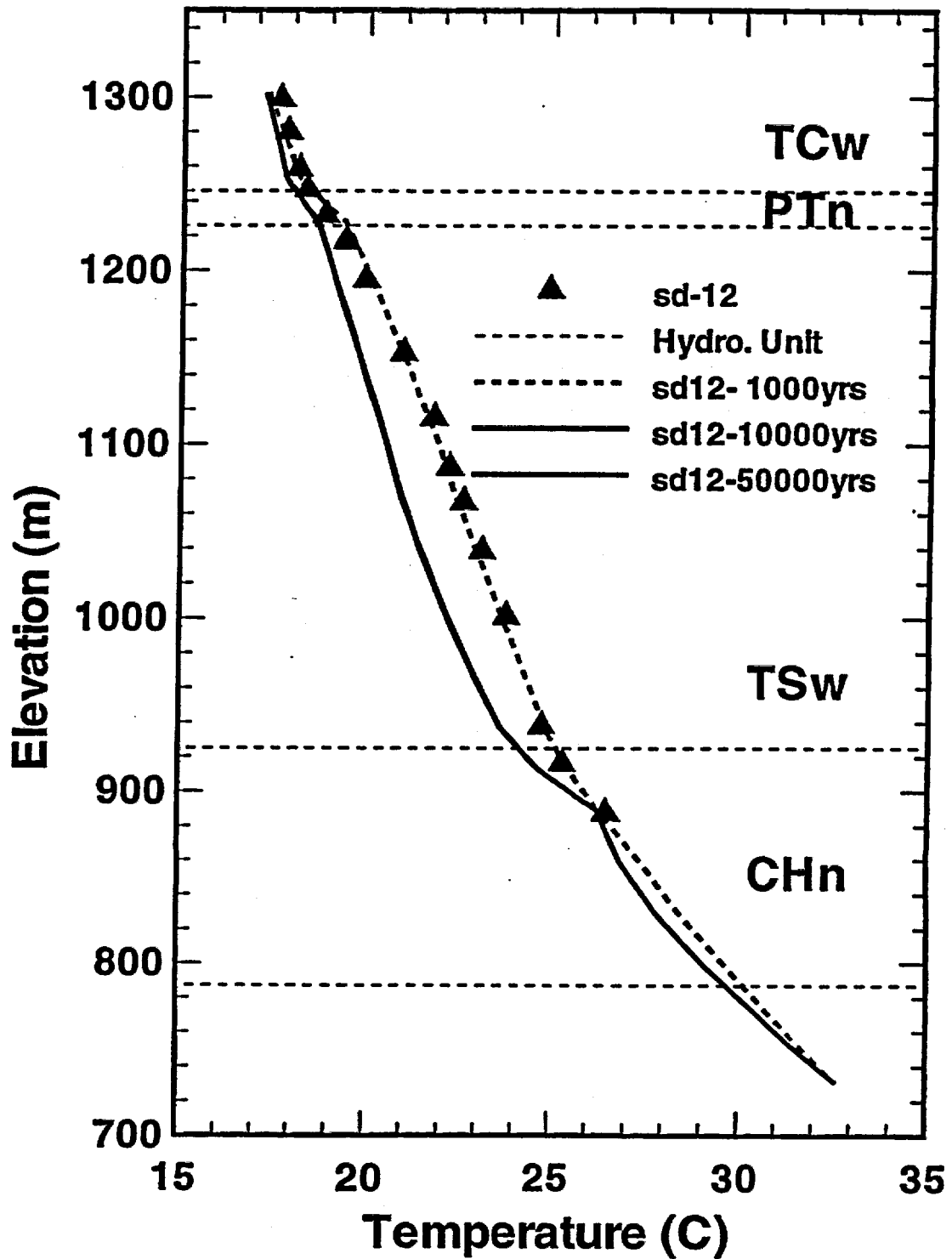
Figure 13: Comparison between observed and modeled temperature profiles at borehole USW SD-12.